

Oxidation of ablated silicon during pulsed laser deposition in a background gas with different oxygen partial pressures

Sergey V. Starinskiy^{1,2*}, *Alexey A. Rodionov*^{1,2}, *Yuri G. Shukhov*¹,
and *Alexander V. Bulgakov*^{1,3}

¹S.S. Kutateladze Institute of Thermophysics SB RAS, Lavrentyev ave. 1, 630090 Novosibirsk, Russia

²Novosibirsk State University, Pirogova Str. 2, 630090, Novosibirsk, Russia

³HiLASE Centre, Institute of Physics of the Czech Academy of Sciences, Za Radnicí 828, 25241 Dolní Břežany, Czech Republic

Abstract. We have analysed changes in the oxidation state of SiO_x films produced by pulsed laser deposition in a background gas with different partial pressures of oxygen. The optical properties of the films in IR range are shown to be close to those of SiO₂ while the total oxidation degree is considerably less than 2. It is suggested that the film consists of oxidized and unoxidized regions due to preferential oxidation of the periphery of the silicon ablation plume during expansion. These regions are overlapping in the film if the laser beam is scanned on the target.

1 Introduction

Silicon suboxide (SiO_x) is a perspective material for various applications, in particular in solar energy converters [1,2]. The material has different properties depending on structure and composition which are largely determined by the method and conditions of its synthesis [3]. Today SiO_x films are obtained by various methods such as HW CVD [3], PE CVD [4], and thermal deposition [5]. The materials can be also produced by pulsed laser deposition (PLD), a method characterized by high purity and exquisite control of the syntheses process [6]. PLD has already been used for SiO_x film deposition [7,8] but mechanisms of silicon oxidation and film structure formation still remain unclear. In this work, we analysed changes in the oxidation state of SiO_x deposited by PLD in a Ar-O₂ background gas mixture with different partial pressure of oxygen. It is demonstrated that properties of the produced films cannot be described within the random bonding model [9]. To explain the obtained results, a film structure consisting of alternating regions with different oxidation degrees is suggested. Processes in the laser ablation plume responsible for the formation of such a structure are discussed.

* Corresponding author: starikhbz@mail.ru

2 Experimental setup and research technique

The films were deposited in a PLD set up described previously [10,11]. In brief, a high purity silicon target was placed in a vacuum chamber (base pressure 1 Pa) and irradiated by a Nd:YAG laser (wavelength 532 nm, pulse duration 7 ns, repetition rate 8 Hz.). The laser beam was focused on the target surface by a 50-cm focal length lens onto a spot area of 0.1 mm^2 to give laser fluence of 12 J/cm^2 . During deposition, the beam was scanned on the target in the horizontal direction along a 17-mm line in order to avoid formation of deep craters on the surface and to ensure the horizontal uniformity of the film. The films were deposited onto crystalline silicon (100) with a native oxide layer. The target-substrate distance and number of laser pulses were 19 mm and 40000, respectively. The ablation was performed in an oxygen – argon background gas mixture. In all cases, the total pressure of the gas was 60 Pa, while the partial pressure of oxygen P_{O_2} was varied in range 0.5-60 Pa. The surface morphology and the thickness of the obtained films were determined by Scanning Electron Microscopy (SEM) using a JEOL JSM-6700F microscope. The composition properties of the SiO_x films were studied by Fourier Transform Infrared spectroscopy (FTIR). The FTIR measurements were carried out in the $2000\text{-}800 \text{ cm}^{-1}$ range using a Scimitar FTS 2000 spectrophotometer.

3 Results and discussion

Typical SEM images of the deposited films are presented in Fig. 1. The morphology of the films is rather complicated and consists of two kinds of sub-structures. There are relatively large particulates with an average size of about several hundred of nanometers around which porous structures are formed. The surface morphologies of the films deposited at different oxygen partial pressures are basically similar with, however, a higher porosity for higher P_{O_2} values (see insets in Fig. 1). Low content of oxygen results in fusion of porous structures (Fig. 1,a) while for higher oxygen pressure one can see individual porous regions with clear boundaries. This dependence is confirmed with cross-sectional SEM analysis showing that the thickness of the films increases with increasing the oxygen partial pressure (Figs. 1,d-f). Since the density of bulk silicon and silicon oxides are almost identical, this indicates a decreasing film density with the oxygen content. Note that, due to the equal total pressure of the background gas, the laser ablation plume propagation into the gas mixture with different oxygen concentration is similar [12] and thus the same amount of silicon is expected to be deposited for all the considered conditions.

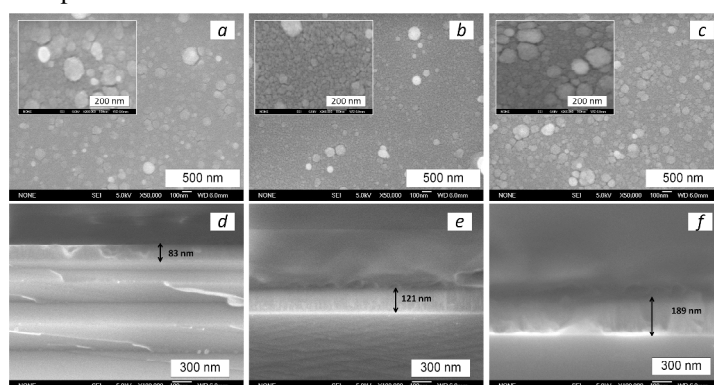


Fig. 1. Planar (top row) and cross-section (bottom row) SEM images of SiO_x films deposited at $P_{\text{O}_2} = 0.5 \text{ Pa}$ (a,d), 30 Pa (b,e) and 60 Pa (c,f). The insets show the same planar images with a higher magnification.

The oxygen content for the deposited films was determined by the FTIR method. The IR transmittance spectra of the films deposited at different P_{O_2} pressures are presented in Fig. 2.a. The transition from the transmittance T to the absorption coefficient α is performed by equation [10]:

$$\alpha = \frac{1}{d} \ln \left[\frac{\frac{T}{T_0}(1-T_0)^2}{-2T_0 + \sqrt{4T_0^2 + \frac{T^2}{T_0^2}(1-T_0^2)^2}} \right], \quad (1)$$

where d is the film thickness, T_0 is the transmittance of the silicon substrate. Results of the transformation are presented in Fig. 2.b. The observed absorption peak is associated with the Si-O-Si stretching mode [13] and its position ω_p is shifted from 1043 cm^{-1} to 1067 cm^{-1} with increasing in P_{O_2} from 0.5 to 60 Pa. According to the random bonding model [9], the stoichiometric coefficient x can be estimated as [12]:

$$x = \frac{\omega_p - 965}{50} \quad (2).$$

The calculated dependence of the stoichiometric coefficient on the oxygen partial pressure is presented in Fig. 3.a. The film is almost completely oxygenated, even for the case of half the oxygen content in the background gas.

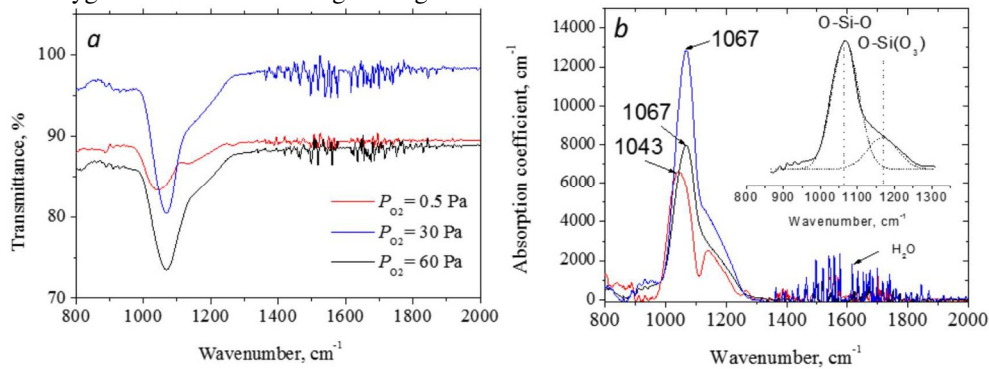


Fig. 2. a) FTIR spectra of SiO_x films deposited at different P_{O_2} pressures. b) Absorption coefficients of the same films calculated by Eq. (1). The inset shows the Gaussian deconvolution of the absorption peak for $P_{O_2} = 60 \text{ Pa}$ into probable satellite components.

On the other hand, the atomic oxygen concentration in the films can also be calculated from the expression [13]:

$$x = \frac{N_o}{N_{Si}}, \quad (3)$$

$$N_o = A_o \cdot \int \frac{\alpha(\omega)}{\omega} d\omega, \quad (4)$$

where $N_{Si} = 5 \times 10^{22} \text{ cm}^{-3}$ is the atomic density of crystalline silicon, and the proportionality constant $A_o = 1.48 \times 10^{19} \text{ cm}^{-2}$. The stoichiometric coefficients calculated from Eqs. (3,4) are presented in Fig. 3.a. In these calculations, we have taken into account the decreasing silicon concentration with increase in the partial oxygen pressure in proportion to the film thickness (Fig. 1), assuming the total amount of silicon in the film to be independent on the oxygen concentration in the background gas. Wherein silicon concentration of dense film (Fig. 1.a,d) taken equal to the atomic density of crystalline silicon mentioned above. The obtained values are considerably lower than those calculated from Eq. (2). This is probably due to the fact that the expression (2) is applicable only for the random bonding model which apparently does not correspond to the produced film structure.

To explain the inconsistency in the oxygen contents determined using the two different ways, we suggest the following mechanism of SiO_x film formation during PLD. When the laser plume expands, only its periphery reacts with the background oxygen while the core remains unoxidized (Fig. 3,b). The size of the core is determined by the penetration depth of background gas molecules into the laser plume and depends on the total gas pressure. In its turn, the periphery oxidation degree depends on the oxygen partial pressure and its complete oxidation is observed already at $P_{\text{O}_2} = 30$ Pa. As a result, oxidized and unoxidized regions are formed in the film during PLD. The scanning of laser beam leads to overlapping of these regions. Therefore, oxygen atoms are inserted in silicon bonds not on a random basis. Instead, the film consists of alternating regions with strongly different oxidation degrees where the compositions are close to Si and SiO_2 (Fig. 3,b). The completely oxidized regions absorb light in the absorption band of SiO_2 that determines the position of the peaks in the FTIR spectra. However, since not all silicon is oxidized in the film the effective stoichiometric coefficient x is considerably smaller than 2.

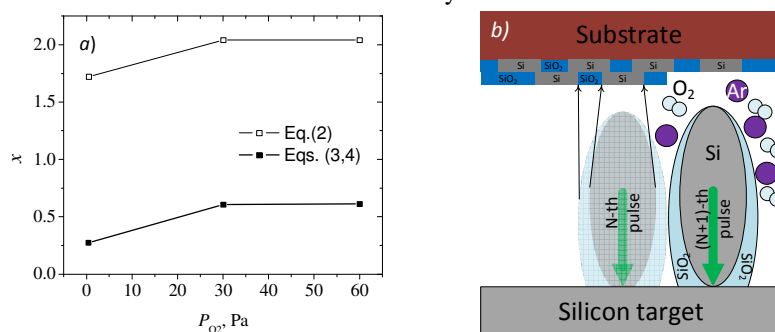


Fig. 3. a) Dependence of the stoichiometric coefficient x of SiO_x on the oxygen partial pressure. b) Scheme of uneven oxidation of the deposited film.

Conclusions

We show that nanosecond PLD of silicon films in an oxygen-containing background gas is characterized not only by an increase in the degree of oxidation of the film but also by a decrease in its density. It is shown that the model of random bonding cannot describe the synthesized material. An explanation is proposed which assumes that the films consist of oxygen enriched areas and areas of pure silicon due to preferential oxidation of the laser plume periphery without affecting the plume core. Scanning the laser beam over the target results in overlapping the oxidized and unoxidized regions.

This work was supported by the Russian Science Foundation (project No. 16-19-10506, film depositions) and by the ERDF and the state budget of the Czech Republic (project BIATRI: No. CZ.02.1.01/0.0/0.0/15_003/0000445, film characterization).

References

1. R.S. Bonilla, B. Hoex, P. Hamer, P.R. Wilshaw, *Phys. Status Solidi* **214**, 1 (2017).
2. S. Wang, V. Smirnov, T. Chen, B. Holländer, X. Zhang, S. Xiong, Y. Zhao, F. Finger, *Jpn. J. Appl. Phys.* **54**, 011401 (2015).
3. A. Ledermann, U. Weber, C. Mukherjee, B. Schroeder, *Thin Solid Films* **395**, 61 (2001).
4. A.H. Mahan, J. Carapella, B.P. Nelson, R.S. Crandall, I. Balberg, *J. Appl. Phys.* **69**, 6728 (1991).

5. D. Nesheva, I. Bineva, Z. Levi, Z. Aneva, T. Merdzhanova, J.C. Pivin, *Vacuum* **68**, 1 (2003).
6. D. Bäuerle, *Laser Processing and Chemistry* (Springer-Verlag, Berlin Heidelberg, 2011).
7. E. Fazio, E. Barletta, F. Barreca, F. Neri, S. Trusso, *J. Vac. Sci. Technol. B* **23**, 519 (2005).
8. N. Saxena, A. Agarwal, D. Kanjilal, *Phys. B* **406**, 2148 (2011).
9. H.R. Philipp, *J. Non. Cryst. Solids* **8–10**, 627 (1972).
10. S.V. Starinskiy, Y.G. Shukhov, A.V. Bulgakov, *Tech. Phys. Lett.* **42**, 411 (2016).
11. M. Jdraque, A.B. Evtushenko, D. Ávila-Brandé, M. López-Arias, V. Lorient, Y.G. Shukhov, L.S. Kibis, A.V. Bulgakov, M. Martín, *J. Phys. Chem. C* **117**, 5416 (2013).
12. A.V. Bulgakov, N.M. Bulgakova, *J. Phys. D.* **31**, 693 (1998).
13. E. Baranov, S. Khmel, A. Zamchiy, M. Buyko, *Phys. Status Solidi* **213**, 1783 (2016).